

Topological Excitations in Two-Dimensional Superconductors

S. Doniach

Department of Applied Physics, Stanford University, Stanford, California 94305

and

B. A. Huberman

Xerox Palo Alto Research Center, Palo Alto, California 94305

(Received 2 February 1979)

We propose a method to calculate the unbinding of a gas of thermally activated vortex pairs above a critical temperature T_{2D} lying below the bulk transition temperature T_{BCS} of thin superconducting films, as a function of temperature and applied magnetic field. We hence determine the phase diagram of the films and their resistivity as a function of field and temperature.

It has been pointed out by Beasley, Mooij, and Orlando¹ that thin-film dirty superconductors whose normal-state resistivity is an appreciable fraction of a "maximum metallic resistivity" (of order 34 000 Ω per square) have a transverse penetration depth $\lambda_{\perp} = \lambda^2/d$ (with λ the London parameter and d the film thickness) which can be comparable to the sample size, R . Under these conditions, thermally excited vortex pairs interact via a two-dimensional Coulomb force law given (for $r \ll \lambda_{\perp}$) by

$$U_{ij} = -2q_i q_j \ln(r_{ij}/\xi), \quad (1)$$

where $q^2 = (\varphi_0/4\pi)^2 \lambda_{\perp}^{-1}$ measures an effective charge for the vortices, φ_0 is the flux quantum ($hc/2e$), and ξ is the core radius. As shown by Berezinskii,² and by Kosterlitz and Thouless,³ a gas of thermal topological excitations of this type is expected to have a finite condensation energy temperature, $T_{2D} < T_{BCS}$ below which the pairs become bound. Moreover, since free vortices will be swept across the sample by a finite current, these superconductors should exhibit a finite resistivity for $T < T_{BCS}$, decreasing to zero as $T \rightarrow T_{2D}$.

The purpose of this Letter is to establish the phase diagram of this class of two-dimensional superconductors in the magnetic-field-temperature plane, and to give a method of calculation of the dependence of their resistivity on temperature, applied field, and current. The same method enables us to calculate the magnetization of the superconducting film.

The effective Hamiltonian of a system of vortices in a superconducting film may be written, following Pearl,⁴ as

$$\mathcal{H} = N\mu_0 + U_0 \left| \sum_i \text{sgn}(q_i) \right|^2 + \frac{1}{2} \sum_{i \neq j} U_{ij} + H \sum_i m_i, \quad (2)$$

where N is the total number of vortices, μ_0 is the chemical potential associated with the vortex core ($\mu_0 = d\xi^2 H_c^2/8$), U_0 is the magnetic energy associated with an excess of vortices of a given sign, which is given by

$$U_0 = q^2 \ln(R/\xi), \quad (3)$$

and m_i is the paramagnetic moment of the i th vortex, $m_i = m \text{sgn}(q_i)$, where

$$M = (\varphi_0/16\pi)(R^2/\lambda_{\perp}). \quad (4)$$

In the spirit of the Kosterlitz and Thouless theory,³ under conditions of large μ_0 (leading to a low density of vortex pairs) a distance-dependent dielectric function $\epsilon(r, T)$ may be defined in the temperature range $0 < T < T_{2D}$; in terms of which the transition temperature T_{2D} can be defined as

$$K_B T_{2D} = q^2/2 \epsilon(\infty, T_{2D}) \quad (5)$$

with $\epsilon(\infty, T_{2D})$ of order unity. Writing the effective charge of the vortex in terms of the film parameters, Eq. (5) can be expressed as $K_B T_{2D} \simeq (\varphi_0/4\pi)^2/2\lambda_{\perp}$ which, as shown by Beasley, Mooij, and Orlando,¹ leads to an expression relating T_{2D}/T_{BCS} to the ratio of the normal-state resistivity of the film to the "maximum metallic resistivity." (E.g., they find $T_{2D}/T_{BCS} \simeq 0.75$ for a film with $R_{\square} = \rho_n/d \sim 8000 \Omega$, where ρ_n is the normal-state resistivity.)

In order to discuss the effects of temperature and applied field on the superconducting properties of thin films, we first look at the phase diagram of a system described by Eq. (2). At $T=0$, the field H_{c1} for which the film becomes unstable to the nucleation of a single vortex is given by the ratio $(\mu_0 + U_0)/m$. Using Eqs. (3) and (4) we obtain the size-dependent value $H_{c1} \simeq 4\varphi_0 R^{-2} \ln(R/\xi)$, which is of order 10^{-5} G for $R \sim 1$ cm and $\xi \simeq 20 \text{ \AA}$. For $0 < T < T_{2D}$, the nucleation energy for

a single vortex will be lowered because of the finite polarizability of the gas of bound, thermally excited vortex pairs, which interact with the nucleated vortex through the third term of Eq. (2). With the resulting correction to the magnetic energy U_0 , we then get³

$$U = U_0 + (2\pi)^{-1} \int_{\xi}^R d^2r r^{-2} q^2 [\epsilon^{-1}(r) - 1], \quad (6)$$

which implies $U = q^2 \ln(R/\xi)/\epsilon(\infty, T)$. We therefore obtain a renormalized critical field \tilde{H}_{c1} , such that $\tilde{H}_{c1}/H_{c1} = \epsilon^{-1}(\infty, T)$ for $T \leq T_{2D}$. If the effects of the finite sample size on the dielectric behavior predicted for the infinite system are ignored, this quantity may be expected to display the same universal behavior near T_{2D} predicted for the superfluid-density jump in the neutral superfluid.⁵ At T_{2D} , the vortex pairs of largest separation become unbound and it will be argued below that the resulting screening will lead to a reduction of \tilde{H}_{c1} to zero for $T > T_{2D}$. Finally, as the field is further increased, the BCS superconducting order parameter is reduced to zero at the depairing field H_{c2} , leading to the phase diagram shown in Fig. 1.

In the figure, Phase I denotes the weakly diamagnetic superconductor with almost no free vortices present.⁶ In this phase, vortex depairing can occur in the presence of a current, thus leading to a resistivity varying as a power of the current. This mechanism is analogous to that found in the ⁴He films.⁷ Phase II corresponds to a superconductor with a screening vortex plasma. The finite polarizability of this phase leads to a strong temperature and field dependence of the resistivity. As Phase III is approached from below the phase boundary, amplitude and phase fluctuations of the BCS condensate become important, and above the depairing field H_{c2} , one obtains a normal metal.

For applied fields larger than \tilde{H}_{c1} for $T < T_{2D}$, or in all finite fields at $T > T_{2D}$, the superconducting film will always have finite density of unbound vortices, $n_{\pm}(T, H)$ with paramagnetic moments parallel (+) or antiparallel (-) to the field, respectively. These free vortices will be swept towards the film boundaries by a current flow, thereby leading to a finite resistivity $\rho(T, H)$ which can be written as⁸

$$\rho(T, H)/\rho_n = 2\pi\xi^2(n_+ + n_-). \quad (7)$$

Therefore, in order to calculate the resistivity and magnetization of the superconductor in the vortex-plasma region of the phase diagram, we need an expression for the temperature- and

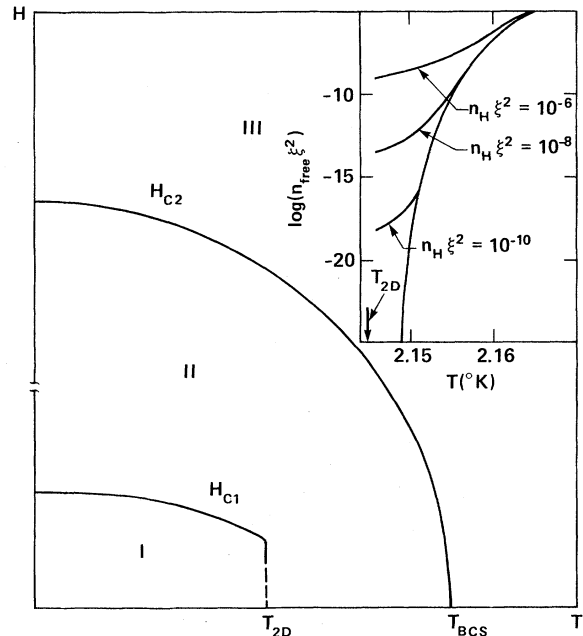


FIG. 1. Phase diagram of a two-dimensional superconductor (not drawn to scale). Phase I denotes the weakly diamagnetic superconductor with almost no free vortices present. H_{c1} is the nucleation field appropriate to a thin film (in the region of 10^{-5} Oe). Phase II contains a screening vortex plasma. Phase III corresponds to the normal state, with H_{c2} the depairing field (of order of kilo-oersteds). Inset: Solution of Eqs. (14) and (15) for $H = 0$ and in the charging limit, $H \gg H_{\text{crossover}}$. The parameters used were $x = 0$ [see Eq. (11)] and $2e^{-\beta\tilde{\mu}_0} = 0.95$. $n_H = 2H/[\pi R^2 H_{c1}(0)]$.

field-dependent densities of unbound vortices.

In order to calculate the density of free vortices, we first notice that in Phase II the vortex plasma will exhibit screening behavior at distances of the order of the screening length κ^{-1} which, in linear-response theory, is given by

$$\kappa^2 = (2\pi/K_B T)(n_+ + n_-)q^2. \quad (8)$$

Consider now the energy $2U^\infty$, associated with injecting a pair of vortices into the film whose separation is much larger than κ^{-1} . Since each vortex of the additional pair will only polarize the bound-pair component of the plasma up to a distance κ^{-1} , we postulate, in a similar vein as Kosterlitz and Thouless,³ that U^∞ scales with κ^{-1} in the low-density limit as

$$U^\infty = [q^2/\epsilon(\kappa^{-1}, T)] \ln(C/\kappa\xi) \quad (9)$$

with C an arbitrary constant. We now show that in zero applied field, Eq. (9) leads to the free-

vortex density found by Kosterlitz from renormalization-group arguments.³ This follows by assuming that as $T \rightarrow T_{2D}^+$, $\epsilon(\kappa^{-1}, T)$ varies as $\epsilon(\infty, T_{2D})\{1+x[(T/T_{2D})-1]^{1/2}\}$, where x is a numerical constant which will, in general, be expected to depend on the bound-vortex density (i.e., μ_0). We then calculate $n_+ = n_- = \frac{1}{2}n_{free}$ self-consistently in the zero-field limit as

$$n_{free} = 2\xi^{-2} \exp(-\beta\mu_0) \exp(-\beta U^\infty) \quad (10)$$

which, together with Eq. (9), yields

$$n_{free} = 2\xi^2 [\exp(-\beta\tilde{\mu}_0)]^{\nu(T)}, \quad (11)$$

where $\nu(T) = 1/(t+x t^{1/2})$ with $t = [(T/T_{2D}) - 1]$ and $\tilde{\mu}_0 \cong \mu_0 + \ln(C^2/\pi)$. Our scaling postulate (9)

$$U_{charging} = q^2(n_+ - n_-) \left\{ 2\pi R^2 \ln(R/\xi) - \int_\xi^R d^2r \ln(r/\xi) \right\}. \quad (12)$$

or equivalently

$$U_{charging} \cong q^2(n_+ - n_-) \frac{1}{2}(3\pi R^2) \ln(R/\xi).$$

Using Eqs. (3), (9), and (12), we then obtain

$$U_\pm = \mu_0 + U^\infty \mp mH \pm m_B M, \quad (13)$$

where $M = \pi R^2(n_+ - n_-)$ measures the vortex imbalance and $m_B = \frac{1}{2}(3q^2) \ln(R/\xi)$. Writing $n_\pm = \xi^{-2} \exp(-\beta U_\pm)$ we can then calculate the magnetization and free-vortex density for the superconductor, which are given by the solutions of the pair of self-consistent equations

$$M = \pi R^2 n_{free} \sinh\beta(mH - m_B M), \quad (14)$$

$$n_{free} = 2\xi^{-2} [\exp(-\beta\tilde{\mu}_0) \cosh\beta(mH - m_B M)]^{\nu(T)}, \quad (15)$$

valid for $T > T_{2D}$. From these equations we see that for small fields the thin-film diamagnetism is reduced exponentially with H until a crossover region is reached:

$$H_{crossover} \cong H_{c1} \left\{ \ln\left(\frac{1}{\kappa\xi}\right) \left[\ln\left(\frac{R}{\xi}\right) \right]^{-1} \right\}.$$

Beyond $H_{crossover}$ the compensation of the diamagnetism by injected vortices will be limited by the charging effects described in Eq. (12) and for large fields (but still $\ll H_{c2}$) will take the asymptotic form discussed by Pearl.⁴

The increase of free-vortex density caused by the presence of an external field also leads to a strong dependence of the film resistivity on the applied field, a fact that is observed experimentally,¹⁰ and, in particular, exhibits a strong temperature dependence, due to the stimulated unbinding of the bound vortex-antivortex pairs, which explains the character of the observed dependence of resistivity on weak applied magnetic fields (see inset of Fig. 1). Further details on

therefore leads to an essential singularity for n_{free} at T_{2D} , of a form which crosses over from Kosterlitz scaling³ at $t \rightarrow 0$ to Zittartz scaling⁹ for $t \gg x^2$.

In the presence of an externally applied magnetic field, the energy required to inject vortices with paramagnetic moment parallel to the field (+) will be lower than that required for antiparallel (-) vortices, resulting in a net imbalance $n_+ - n_- > 0$ for all nonzero fields, leading to $\tilde{H}_{c1} = 0$ at $T > T_{2D}$. Although the field of each vortex is shielded locally within a distance κ^{-1} the net paramagnetic moments add up over long distances. Hence, in analogy with the charging up of the Coulomb gas, an extra contribution to the energy needed to insert a +vortex into the field will now be given by

these will be given elsewhere.

In conclusion, we have shown that thin superconducting films display novel behavior when their transport and magnetic properties are analyzed as a function of temperature and magnetic field, thus enlarging the range of phenomena generated by topological excitations in neutral superfluids.¹¹

We would like to thank M. R. Beasley, J. E. Mooij, and T. Orlando for telling us about their work in advance of publication, and for many helpful discussions and suggestions. We also thank D. Fisher, A. Luther, and B. Halperin for useful comments.

¹M. R. Beasley, J. E. Mooij, and T. P. Orlando, preceding Letter [Phys. Rev. Lett. **42**, 1165 (1979)], and private communication.

²V. L. Berezinskii, Zh. Eksp. Teor. Fiz. **61**, 1144

(1972) [Sov. Phys. JETP **34**, 610 (1972)],

³J. M. Kosterlitz and D. Thouless, J. Phys. C **6**, 1181 (1973); J. M. Kosterlitz, J. Phys. C **7**, 1046 (1974).

⁴J. Pearl, in *Low Temperature Physics-LT9*, edited by J. G. Daunt, D. O. Edwards, F. J. Milford, and M. Yagub (Plenum, New York, 1965), p. 566.

⁵D. Nelson and J. M. Kosterlitz, Phys. Rev. Lett. **39**, 1201 (1977).

⁶In practice, the finite sample size will lead to a very small, though finite, probability that thermally excited free vortices could occur in Phase I, and similarly for samples $R \geq \lambda_1$.

⁷B. A. Huberman, R. J. Myerson, and S. Doniach, Phys. Rev. Lett. **40**, 780 (1978); V. Ambegaokar, B. I.

Halperin, D. R. Nelson, and E. Siggia, Phys. Rev. Lett. **40**, 783 (1978).

⁸M. Tinkham, *Introduction to Superconductivity* (McGraw-Hill, New York, 1975).

⁹J. Zittartz, Z. Phys. **23**, 55 (1976); H. V. Everts and W. Koch, Z. Phys. B **28**, 117 (1977). This scaling behavior has been recently confirmed by G. Grinstein, P. Minnhagen, and A. Rosengren, to be published.

¹⁰See, for example, W. E. Masker, S. Marčelja, and R. D. Parks, Phys. Rev. **188**, 745 (1969).

¹¹After completion of this work, we received a report from B. I. Halperin and D. R. Nelson, J. Low Temp. Phys. (to be published), in which similar conclusions are independently put forward concerning the finite resistivity in zero applied field.

M-Series Soft-X-Ray Appearance-Potential Spectroscopy of Yb₂O₃

W. E. Harte and P. S. Szczepanek

Laboratory for Physical Sciences, College Park, Maryland 20740

(Received 7 February 1979)

The $M_{5,4}$ soft-x-ray appearance-potential spectrum of Yb₂O₃ does not show the intense structure characteristic of the lighter rare-earth elements even though a single 4*f* vacancy exists in Yb₂O₃. This indicates that the strong $M_{5,4}$ spectral response of each rare-earth element previously measured using the soft-x-ray appearance potential technique is determined primarily by the availability of vacant 4*f* atomic states to accept both the excited *d* electron and the incident electron.

Recently measurements have been made¹⁻¹⁵ of the electron-excited soft-x-ray emission spectra of the rare-earth elements. Characteristic of these investigations have been the intense signals for the $M_{5,4}$ and $N_{5,4}$ spectra. The x-ray emission spectra of La and Ce measured by Liefeld and co-workers^{1,2} revealed a dramatic resonance in bremsstrahlung radiation when the energy of the incident electron was comparable to the excitation threshold for the M_5 and M_4 core-level transitions. Harte, Szczepanek, and Leyendecker⁵ showed that the strong structure in their La and Ce data, obtained using the soft-x-ray appearance-potential (SXAP) technique, was a manifestation of this same bremsstrahlung resonance. The interpretations given of the $M_{5,4}$ SXAP spectra of other rare-earth elements indicates wide variation in the extent to which this resonance is assumed to contribute to each emission spectrum. Our measurements of the Yb₂O₃ $M_{5,4}$ SXAP spectrum indicate that the bremsstrahlung resonance is the dominant contribution in the lighter rare-earth spectra.

Wendin¹⁶ has proposed that, for elements in which a localized excited level exists at energies

near the threshold of a characteristic core excitation, there are three competing transitions which determine the SXAP spectra. The scattering of the incident electron into this empty *f* state [process (a)] gives rise to the normal bremsstrahlung peak. In the second process [process (b)] an intermediate state consisting of the scattered incident electron in a localized atomic 4*f* state together with a second 4*f* electron excited from an atomic 3*d* state, relaxes via photon emission into a final state identical to that of process (a). The exchange interaction involving the 3*d* hole and two 4*f* electrons splits the intermediate-state energy, causing a multiplicity of reaction channels connecting initial and final states. The addition of the transition probabilities associated with these channels together with that of process (a) produce a transition resonance. The third [process (c)], is the inelastic scattering of the incident electron into an itinerant-electron state accompanied by the excitation of an atomic 3*d* electron into a localized 4*f* state. The strong exchange interaction involving the excited 4*f* electron and core hole has been shown by Sugar¹⁷ to lead to considerable multiplicity in the process